











TECH BRIEFS

NATIONAL AERONAUTICS AND SPACE ADMINISTRATION

-  **Technology Focus**
-  **Electronics/Computers**
-  **Software**
-  **Materials**
-  **Mechanics/Machinery**
-  **Manufacturing**
-  **Bio-Medical**
-  **Physical Sciences**
-  **Information Sciences**
-  **Books and Reports**

INTRODUCTION

Tech Briefs are short announcements of innovations originating from research and development activities of the National Aeronautics and Space Administration. They emphasize information considered likely to be transferable across industrial, regional, or disciplinary lines and are issued to encourage commercial application.

Availability of NASA Tech Briefs and TSPs

Requests for individual Tech Briefs or for Technical Support Packages (TSPs) announced herein should be addressed to

National Technology Transfer Center

Telephone No. (800) 678-6882 or via World Wide Web at www2.nttc.edu/leads/

Please reference the control numbers appearing at the end of each Tech Brief. Information on NASA's Innovative Partnerships Program (IPP), its documents, and services is also available at the same facility or on the World Wide Web at <http://ipp.nasa.gov>.

Innovative Partnerships Offices are located at NASA field centers to provide technology-transfer access to industrial users. Inquiries can be made by contacting NASA field centers listed below.

NASA Field Centers and Program Offices

Ames Research Center

Lisa L. Lockyer
(650) 604-1754
lisa.l.lockyer@nasa.gov

Dryden Flight Research Center

Gregory Poteat
(661) 276-3872
greg.poteat@dfrc.nasa.gov

Glenn Research Center

Kathy Needham
(216) 433-2802
kathleen.k.needham@nasa.gov

Goddard Space Flight Center

Nona Cheeks
(301) 286-5810
nona.k.cheeks@nasa.gov

Jet Propulsion Laboratory

Ken Wolfenbarger
(818) 354-3821
james.k.wolfenbarger@jpl.nasa.gov

Johnson Space Center

Michele Brekke
(281) 483-4614
michele.a.brekke@nasa.gov

Kennedy Space Center

David R. Makufka
(321) 867-6227
david.r.makufka@nasa.gov

Langley Research Center

Martin Waszak
(757) 864-4015
martin.r.waszak@nasa.gov

Marshall Space Flight Center

Jim Dowdy
(256) 544-7604
jim.dowdy@msfc.nasa.gov

Stennis Space Center

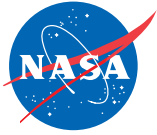
John Bailey
(228) 688-1660
john.w.bailey@nasa.gov

Carl Ray, Program Executive

Small Business Innovation
Research (SBIR) & Small
Business Technology
Transfer (STTR) Programs
(202) 358-4652
carl.g.ray@nasa.gov

Doug Comstock, Director

Innovative Partnerships
Program Office
(202) 358-2560
doug.comstock@nasa.gov



TECH BRIEFS

NATIONAL AERONAUTICS AND SPACE ADMINISTRATION



5 Technology Focus: Test & Measurements

- 5 Optical Measurement of Mass Flow of a Two-Phase Fluid
- 6 Selectable-Tip Corrosion-Testing Electrochemical Cell
- 6 Piezoelectric Bolt Breakers and Bolt Fatigue Testers
- 7 Improved Measurement of B_{22} of Macromolecules in a Flow Cell
- 8 Measurements by a Vector Network Analyzer at 325 to 508 GHz



9 Bio-Medical

- 9 Using Light To Treat Mucositis and Help Wounds Heal



11 Electronics/Computers

- 11 Increasing Discharge Capacities of $\text{Li}(\text{CF})_n$ Cells
- 12 Dot-in-Well Quantum-Dot Infrared Photodetectors
- 13 Integrated Microbatteries for Implantable Medical Devices



15 Software

- 15 Oxidation Behavior of Carbon Fiber-Reinforced Composites
- 15 GIDEP Batching Tool
- 15 Generic Spacecraft Model for Real-Time Simulation

- 15 Parallel-Processing Software for Creating Mosaic Images

- 16 Software for Verifying Image-Correlation Tie Points

- 16 Flexcam Image Capture Viewing and Spot Tracking



17 Materials

- 17 Low-Pt-Content Anode Catalyst for Direct Methanol Fuel Cells

- 17 Graphite/Cyanate Ester Face Sheets for Adaptive Optics

- 18 Atomized $\text{BaF}_2\text{-CaF}_7$ for Better-Flowing Plasma-Spray Feedstock

- 19 Nanophase Nickel-Zirconium Alloys for Fuel Cells



21 Manufacturing & Prototyping

- 21 Vacuum Packaging of MEMS With Multiple Internal Seal Rings



23 Physical Sciences

- 23 Compact Two-Dimensional Spectrometer Optics



25 Information Sciences

- 25 Fault-Tolerant Coding for State Machines

This document was prepared under the sponsorship of the National Aeronautics and Space Administration. Neither the United States Government nor any person acting on behalf of the United States Government assumes any liability resulting from the use of the information contained in this document, or warrants that such use will be free from privately owned rights.



Optical Measurement of Mass Flow of a Two-Phase Fluid

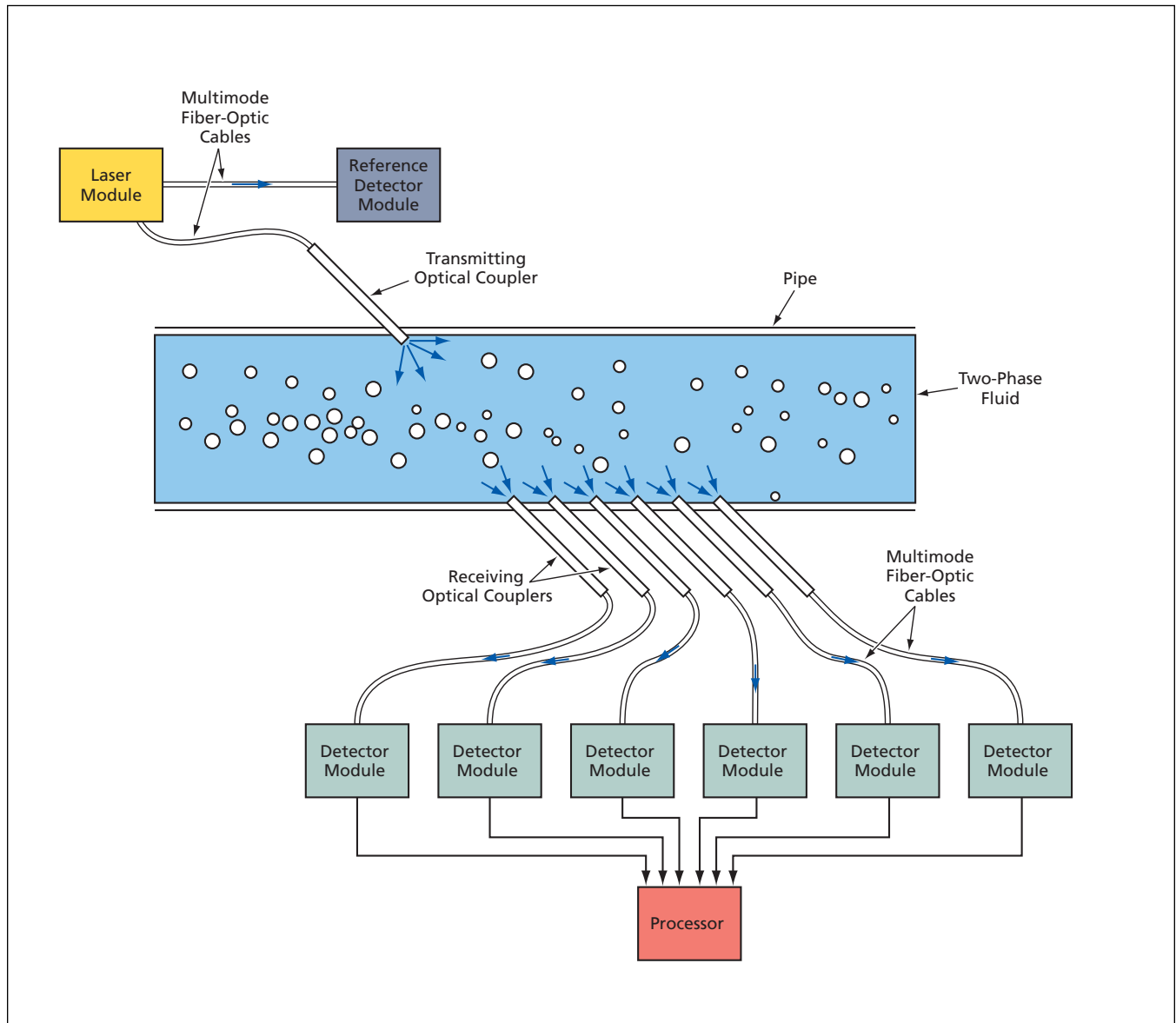
Density and mass flow are estimated from wavelength-dependent scattering of light.

Marshall Space Flight Center, Alabama

An optoelectronic system utilizes wavelength-dependent scattering of light for measuring the density and mass flow of a two-phase fluid in a pipe. The apparatus was invented for original use in measuring the mass flow of a two-phase cryogenic fluid (e.g., liquid hydrogen containing bubbles of hydrogen gas), but underlying principles of operation can readily be adapted to non-cryogenic two-phase fluids.

The system (see figure) includes a laser module, which contains two or more laser diodes, each operating at a different wavelength. The laser module also contains beam splitters that combine the beams at the various wavelengths so as to produce two output

beams, each containing all of the wavelengths. One of the multiwavelength output beams is sent, via a multimode fiber-optic cable, to a transmitting optical coupler. The other multiwavelength output beam is sent, via another multimode fiber-optic cable, to a reference detector module, wherein fiber-optic splitters split the light into several multiwavelength



Laser Light at Multiple Wavelengths is introduced into a two-phase fluid in a pipe at one point. After scattering by the fluid, the light is detected at multiple points on the opposite side of the pipe.

beams, each going to a photodiode having a spectral response that is known and that differs from the spectral responses of the other photodiodes. The outputs of these photodiodes are digitized and fed to a processor, which executes an algorithm that utilizes the known spectral responses to convert the photodiode outputs to obtain reference laser-power levels for the various wavelengths.

The transmitting optical coupler is mounted in (and sealed to) a hole in the pipe and is oriented at a slant with respect to the axis of the pipe. The transmitting optical coupler contains a collimating lens and a cylindrical lens that form the light emerging from the end of the fiber-optic cable into a fan-shaped

beam in a meridional plane of the pipe. Receiving optical couplers similar to the transmitting optical couplers are mounted in the same meridional plane at various longitudinal positions on the opposite side of the pipe, approximately facing the transmitting optical coupler along the same slant.

Light collected by each receiving optical coupler is sent, via a multimode fiber-optic cable, to a detector module similar to the reference detector module. The outputs of the photodiodes in each detector module are digitized and processed, similarly to those of the reference detector module, to obtain indications of the amounts of light of each wavelength scattered to the correspon-

ding receiving position. The value for each wavelength at each position is also normalized to the reference laser-power level for that wavelength. From these normalized values, the density and the mass flow rate of the fluid are estimated.

This work was done by John Wiley and Kevin Pedersen of Marshall Space Flight Center; Valentin Korman of Madison Research Corp., and Don Gregory of the University of Alabama at Huntsville.

This invention is owned by NASA, and a patent application has been filed. For further information, contact Sammy Nabors, MSFC Commercialization Assistance Lead, at sammy.a.nabors@nasa.gov. Refer to MFS-32031-1.

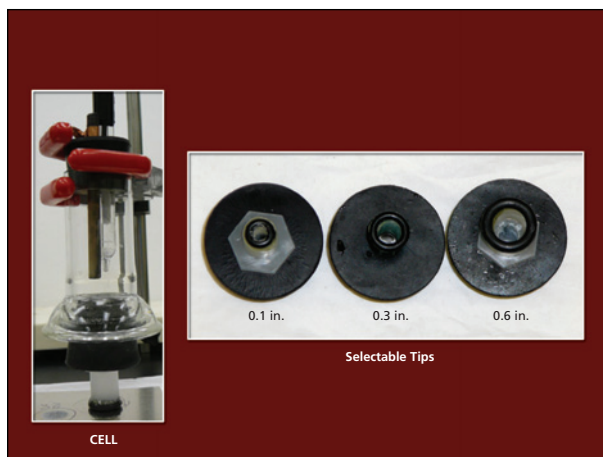
Selectable-Tip Corrosion-Testing Electrochemical Cell

The diameter and average depth of a corrosion pit can be selected.

John F. Kennedy Space Center, Florida

The figure depicts aspects of an electrochemical cell for pitting-corrosion tests of material specimens. The cell is designed to generate a region of corrosion having a pit diameter determined by the diameter of a selectable tip. The average depth of corrosion is controlled by controlling the total electric charge passing through the cell in a test. The cell is also designed to produce minimal artifacts associated with crevice corrosion.

There are three selectable tips, having diameters of 0.1 in. (0.254 cm), 0.3 in. (0.762 cm), and 0.6 in. (1.524 cm), respec-



This Corrosion-Testing Electrochemical Cell is equipped with one of three selectable tips. Each tip features a different corrosion-pit diameter.

tively. The amount of electric charge needed to generate a corrosion pit having desired average depth h at a selected diameter d is given straightforwardly by

$$Q = F\rho\pi d^2 h / (4W)$$

F is the Faraday constant (the charge of one mole of electrons), ρ is the mass density of the specimen material, and W is the equivalent weight of the material (the mass of one mole of the material divided by the valence of the material).

This work was done by Janice Lomness and Paul Hintze of Kennedy Space Center. Further information is contained in a TSP (see page 1). KSC-13045

Piezoelectric Bolt Breakers and Bolt Fatigue Testers

Safer alternative to spacecraft explosive bolts may accelerate fatigue testing on Earth.

NASA's Jet Propulsion Laboratory, Pasadena, California

A proposed family of devices for inducing fatigue in bolts in order to break the bolts would incorporate piezoelectric actuators into resonant fixtures as in ultrasonic/sonic drills/corers and similar devices described in numerous prior *NASA Tech Briefs* articles. These devices were originally intended primarily for use as safer, more-reliable, more-versatile alter-

natives to explosive bolts heretofore used to fasten spacecraft structures that must subsequently be separated from each other quickly on command during flight. On Earth, these devices could be used for accelerated fatigue testing of bolts.

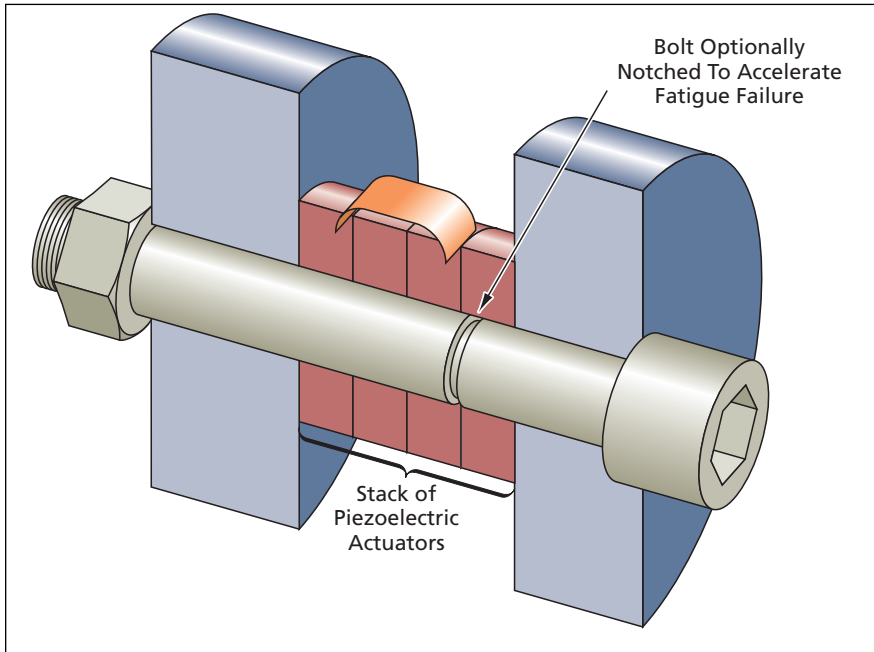
Fatigue theory suggests that a bolt subjected to both a constant-amplitude dynamic (that is, oscillatory) stress and a

static tensile stress below the ultimate strength of the bolt material will fail faster than will a bolt subjected to only the dynamic stress. This suggestion would be applied in a device of the proposed type. The device would be designed so that the device and the bolt to be fatigue-tested or broken would be integral parts of an assembly (see figure).

The static tension in the tightened bolt would apply not only the clamping force to hold the joined structures (if any) together but also the compression necessary for proper operation of the piezo-

electric actuators as parts of a resonant structural assembly. The constant-amplitude dynamic stress would be applied to the bolt by driving the piezoelectric actuators with a sinusoidal voltage at the reso-

nance frequency of longitudinal vibration of the assembly. The amplitude of the excitation would be made large enough so that the vibration would induce fatigue in the bolt within an acceptably short time.



A Bolt To Be Fatigue-Tested or simply broken by accelerated fatigue would be tightened as an integral part of a resonant assembly that would also include piezoelectric actuators that would apply an oscillatory component of tensile stress.

In the spacecraft applications or in similar terrestrial structural-separation applications, devices of the proposed type would offer several advantages over explosive bolts: Unlike explosive bolts, the proposed devices would be reusable, could be tested before final use, and would not be subject to catastrophic misfire. In fatigue-testing applications, devices of the proposed type would offer advantages of compactness and low cost, relative to conventional fatigue-testing apparatuses. In both structural-separation and fatigue-testing applications, bolts to be broken or tested could be instrumented with additional ultrasonic transducers for monitoring of pertinent physical properties and of fatigue failure processes.

This work was done by Stewart Sherrit, Mircea Badescu, Yoseph Bar-Cohen, Jack Barengoltz, and Vanessa Heckman of Caltech for NASA's Jet Propulsion Laboratory. Further information is contained in a TSP (see page 1). NPO-43977

Improved Measurement of B_{22} of Macromolecules in a Flow Cell

Invention helps researchers understand conditions that affect protein crystallization.

Marshall Space Flight Center, Alabama

An improved apparatus has been invented for use in determining the osmotic second virial coefficient of macromolecules in solution. In a typical intended application, the macromolecules would be, more specifically, protein molecules, and the protein solution would be pumped through a flow cell to investigate the physical and chemical conditions that affect crystallization of the protein in question.

Some background information is prerequisite to a meaningful description of the novel aspects of this apparatus. The osmotic second virial coefficient, customarily denoted by the algebraic symbol B_{22} , appears in the equation for the osmotic pressure of a macromolecular solution:

$$\pi = RT\rho(M - 1 + B_{22}\rho + \text{higher-order terms})$$

where π is the osmotic pressure, R is the ideal-gas constant, T is the absolute temperature, ρ is the concentration (more

specifically, the mass density) of the macromolecule solute, and M is the mass of one mole of the solute. The osmotic second virial coefficient quantifies the degree of attraction or repulsion between the macromolecules under various solution conditions. Therefore, this coefficient is a valuable part of a method of determining optimum conditions for formulation of a protein solution and crystallization of the protein from the solution.

A method of determining B_{22} from simultaneous measurements of the static transmittance (taken as an indication of concentration) and static scattering of light from the same location in a flowing protein solution was published in 2004. The apparatus used to implement the method at that time included a dual-detector flow cell, which had two drawbacks:

- The amount of protein required for analysis of each solution condition was of the order of a milligram — far too large a quantity for a high-throughput

analysis system, for which microgram or even nanogram quantities of protein per analysis are desirable.

- The design of flow cell was such that two light sources were used to probe different regions of the flowing solution. Consequently, the apparatus did not afford simultaneous measurements at the same location in the solution and, hence, did not guarantee an accurate determination of B_{22} .

This concludes the background information.

The present improved apparatus includes a flow cell wherein the required simultaneous transmittance and scattering measurements can be made at the same location. For the purpose of these measurements, light from two sources (a laser and an ultraviolet lamp) is delivered simultaneously to the designated location in the cell via a bifurcated optical fiber. The flow cell in this apparatus is narrower than that of the prior appa-

ratus, such that the volume of solution needed for each analysis is of the order of microliters and the mass of protein needed for each analysis at typical concentrations is of the order of micrograms.

The capability of the improved apparatus to yield measurements from

which accurate B_{22} values could be calculated was demonstrated in experiments on several different aqueous lysozyme and concanavalin A solutions for which B_{22} values had been determined by other means. The apparatus has also been used to screen a series of potential crys albumin, and to eval-

uate B_{22} as an indication of the solubility of proteins.

This work was done by Wilbur Wilson, Joseph Fanguy, Steven Holman, and Bin Guo of Mississippi State University for Marshall Space Flight Center. Further information is contained in a TSP (see page 1). MFS-32536-1

Measurements by a Vector Network Analyzer at 325 to 508 GHz

NASA's Jet Propulsion Laboratory, Pasadena, California

Recent experiments were performed in which return loss and insertion loss of waveguide test assemblies in the frequency range from 325 to 508 GHz were measured by use of a swept-frequency two-port vector network analyzer (VNA) test set. The experiments were part of a continuing effort to develop means of characterizing passive and active electronic components and systems operating at ever increasing frequencies. The waveguide test assemblies comprised WR-2.2 end sections collinear with WR-3.3 middle sections. The test set, assem-

bled from commercially available components, included a 50-GHz VNA scattering-parameter test set and external signal synthesizers, augmented with recently developed frequency extenders, and further augmented with attenuators and amplifiers as needed to adjust radio-frequency and intermediate-frequency power levels between the aforementioned components.

The tests included line-reflect-line calibration procedures, using WR-2.2 waveguide shims as the "line" standards and waveguide flange short circuits as the

"reflect" standards. Calibrated dynamic ranges somewhat greater than about 20 dB for return loss and 35 dB for insertion loss were achieved. The measurement data of the test assemblies were found to substantially agree with results of computational simulations.

This work was done by King Man Fung, Lorene Samoska, Goutam Chattopadhyay, Todd Gaier, Pekka Kangaslahti, David Pukala, Yuenie Lau, Charles Oleson, and Anthony Denning of Caltech for NASA's Jet Propulsion Laboratory. For more information, contact iaoffice@jpl.nasa.gov. NPO-44694



Using Light To Treat Mucositis and Help Wounds Heal

Arrays of LEDs would generate biostimulatory radiation.

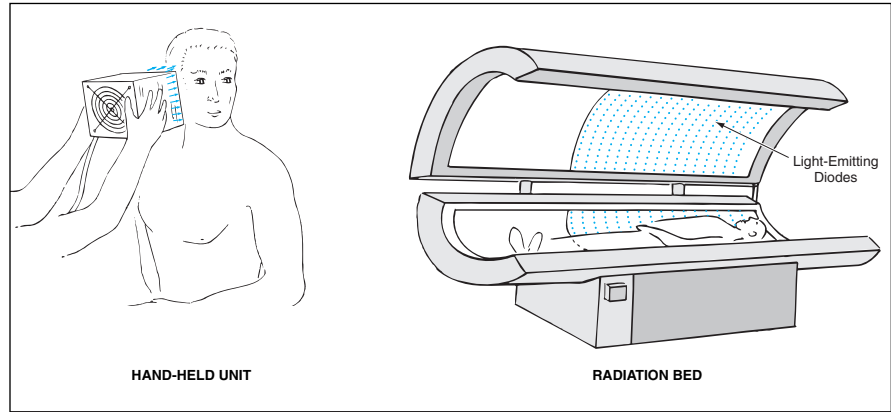
Marshall Space Flight Center, Alabama

A continuing program of research and development is focusing on the use of controlled illumination by light-emitting diodes (LEDs) to treat mucositis and to accelerate healing of wounds. The basic idea is to illuminate the affected area of a patient with light of an intensity, duration, and wavelength (or combination of wavelengths) chosen to produce a therapeutic effect while generating only a minimal amount of heat.

This method of treatment was originally intended for treating the mucositis that is a common complication of chemotherapy and radiation therapy for cancer. It is now also under consideration as a means to accelerate the healing of wounds and possibly also to treat exposure to chemical and radioactive warfare agents.

Radiation therapy and many chemotherapeutic drugs often damage the mucosal linings of the mouth and gastrointestinal tract, leading to mouth ulcers (oral mucositis), nausea, and diarrhea. Hyperbaric-oxygen therapy is currently the standard of care for ischemic, hypoxic, infected, and otherwise slowly-healing problem wounds, including those of oral mucositis. Hyperbaric-oxygen therapy increases such cellular activities as collagen production and angiogenesis, leading to an increased rate of healing. Biostimulation by use of laser light has also been found to be effective in treating mucositis. For hyperbaric-oxygen treatment, a patient must remain inside a hyperbaric chamber for an extended time. Laser treatment is limited by laser-wavelength capabilities and by narrowness of laser beams, and usually entails the generation of significant amounts of heat.

The present method offers an attractive alternative to hyperbaric-oxygen and laser treatments: It is not necessary to confine the patient to a hyperbaric



Apparatuses Containing Arrays of LEDs could range from a hand-held unit for treating oral mucositis to something as large as a radiation bed or a radiation booth (not shown here) for treating mucositis throughout the gastrointestinal tract from the head down through the intestines.

chamber, treatment times are relatively short, LED arrays can illuminate large areas, and the exposure of the patient to heat generated by an LED array can readily be limited.

The figure depicts two examples representative of the range of sizes of treatment apparatuses according to the present method. The preferred sources of light in an apparatus of this type are substantially monochromatic double-heterojunction GaAlAs LEDs arranged in an array large enough to expose the affected area of a patient uniformly at the required intensity. If light of a single wavelength is to be used, then the wavelength believed to be optimal for treating mucositis is 688 nm. If LEDs of 688-nm wavelength are not available, then one could use a three-wavelength combination (680, 730, and 880 nm) that is believed to be an optimal combination for treating mucositis; in this case, the LEDs of the three different wavelengths would be placed side by side in an array. Other single wavelengths and combinations of wavelengths may also be suitable.

In addition to the wavelength(s), the energy density should be chosen to max-

imize the biostimulatory effect. Moreover, the power density must exceed a threshold level in order to exert a biostimulatory effect. The optimal energy density has been determined to be about 4 J/cm^2 . This energy density could be delivered, for example, at a power density of 60 mW/cm^2 (which exceeds the threshold) during an exposure time of 70 seconds. Such a short treatment time is particularly desirable for treating a young child.

This work was done by Robert W. Ignatius, Todd S. Martin, and Charles Kirk of Quantum Devices, Inc. for Marshall Space Flight Center.

In accordance with Public Law 96-517, the contractor has elected to retain title to this invention. Inquiries concerning rights for its commercial use should be addressed to:

*Ronald W. Ignatius, Founder & Chairman
Quantum Devices, Inc.*

*P.O. Box 100
112 Orbison Street
Barneveld, WI 53507*

E-mail: iggyron@quantumdev.com

Refer to MFS-31651, volume and number of this NASA Tech Briefs issue, and the page number.



Increasing Discharge Capacities of Li-(CF)_n Cells

Electrolyte additive could open new applications for Li-(CF)_n batteries.

NASA's Jet Propulsion Laboratory, Pasadena, California

An electrolyte additive has shown promise as a means of increasing the sustainable rates of discharge and, hence, the discharge capacities, of lithium-poly(carbon monofluoride) electrochemical power cells. Lithium-poly(carbon monofluoride) [Li-(CF)_n] cells and batteries offer very high specific energies — practical values of about 600 W·h/g and a theoretical maximum value of 2,180 W·h/kg. However, because Li-(CF)_n cells and batteries cannot withstand discharge at high rates, they have been relegated to niche applications that involve very low discharge currents over times of the order of hundreds to thousands of hours. Increasing the discharge capacities of Li-(CF)_n batteries while maintaining high practical levels of specific energy would open new applications for these batteries.

During the discharge of a Li-(CF)_n cell, one of the electrochemical reactions

causes LiF to precipitate at the cathode. LiF is almost completely insoluble in most non-aqueous solvents, including those used in the electrolyte solutions of Li-(CF)_n cells. LiF is electrochemically inactive and can block the desired transport of ions at the cathode, and, hence, the precipitation of LiF can form an ever-thickening film on the cathode that limits the rate of discharge.

The present electrolyte additive is a member of a class of fluorinated boron-based compounds that function as anion receptors, helping to increase the discharge capacity in two ways:

1. They render LiF somewhat soluble in the non-aqueous electrolyte solution, thereby delaying precipitation until a high concentration of LiF in solution has been reached.
2. When precipitation occurs, they promote the formation of large LiF

grains that do not conformally coat the cathode.

The net effect is to reduce the blockage caused by precipitation of LiF, thereby maintaining a greater degree of access of electrolyte to the cathode.

The fluorinated boron-based anion receptor most commonly used heretofore — tris(pentafluorophenyl) borane — has been found to sharply increase the viscosities of electrolyte solutions. Increases in viscosities generally contribute to reductions in discharge capacities. In contrast, the present additive — tris(hexafluoroisopropyl) borate — can be mixed with such conventional lithium-cell solvents as propylene carbonate and dimethoxyethane to obtain solutions that have much lower viscosities and accept greater concentrations of LiF.

The promise of tris(hexafluoroisopropyl) borate as an additive was demonstrated in an experiment on two Li-(CF)_n cells in standard commercial button-style packages. The cells were identical with one exception: the electrolyte solution in one cell contained 24 weight percent of tris(hexafluoroisopropyl) borate. The cells were tested at discharge currents of 1 mA. As shown in the figure, the cell containing the additive outperformed the one without the additive by a wide margin.

This work was done by Jay Whitacre and William West of Caltech for NASA's Jet Propulsion Laboratory. Further information is contained in a TSP (see page 1).

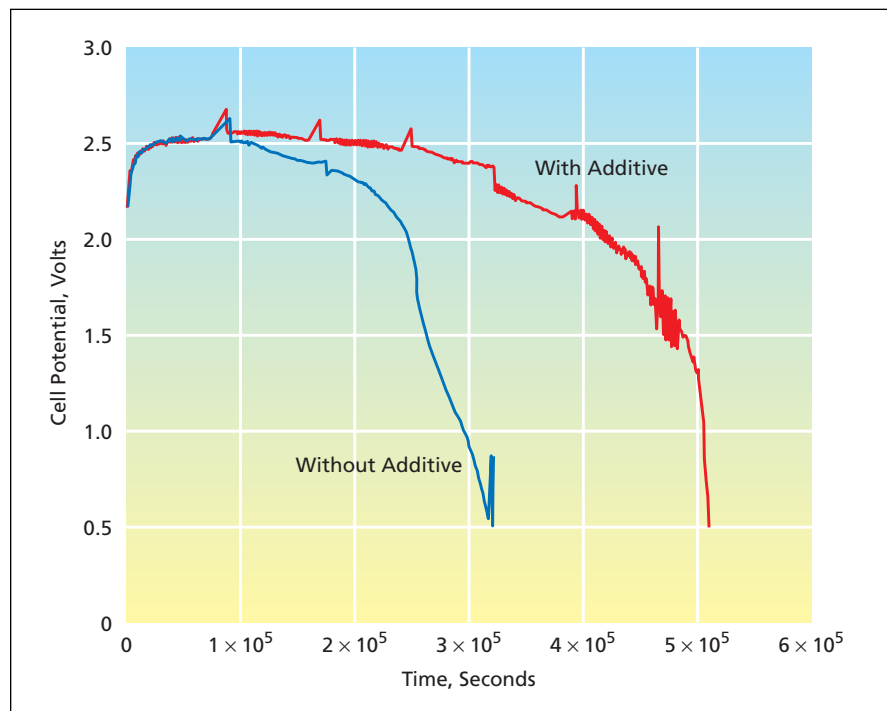
In accordance with Public Law 96-517, the contractor has elected to retain title to this invention. Inquiries concerning rights for its commercial use should be addressed to:

*Innovative Technology Assets Management
JPL*

*Mail Stop 202-233
4800 Oak Grove Drive
Pasadena, CA 91109-8099
(818) 354-2240*

E-mail: iaoffice@jpl.nasa.gov

Refer to NPO-42346, volume and number of this NASA Tech Briefs issue, and the page number.



Potential as a Function of Time was measured in constant-current (1-mA) discharges of two Li-(CF)_n cells that were nominally equivalent except that one contained tris(hexafluoroisopropyl) borate as an electrolyte additive.

Dot-in-Well Quantum-Dot Infrared Photodetectors

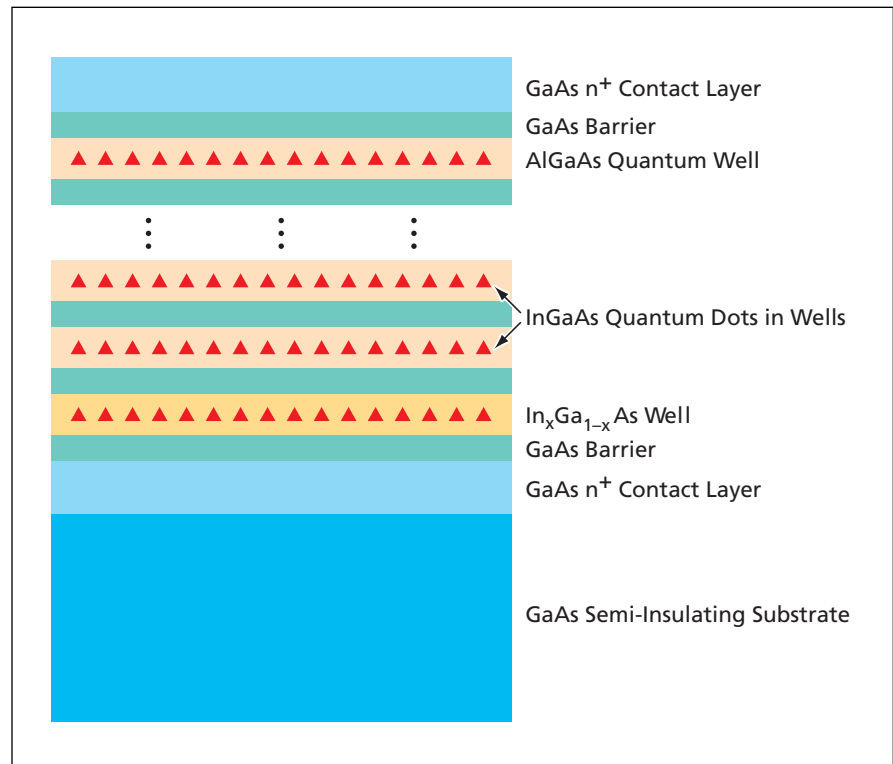
The goal is to develop high-performance radiation-hard QDIPs for focal plane arrays.

NASA's Jet Propulsion Laboratory, Pasadena, California

Dot-in-well (DWELL) quantum-dot infrared photodetectors (QDIPs) [DWELL-QDIPs] are subjects of research as potentially superior alternatives to prior QDIPs. Heretofore, there has not existed a reliable method for fabricating quantum dots (QDs) having precise, repeatable dimensions. This lack has constituted an obstacle to the development of uniform, high-performance, wavelength-tailorable QDIPs and of focal-plane arrays (FPAs) of such QDIPs. However, techniques for fabricating quantum-well infrared photodetectors (QWIPs) having multiple-quantum-well (MQW) structures are now well established. In the present research on DWELL-QDIPs, the arts of fabrication of QDs and QWIPs are combined with a view toward overcoming the deficiencies of prior QDIPs. The longer-term goal is to develop focal-plane arrays of radiation-hard, highly uniform arrays of QDIPs that would exhibit high performance at wavelengths from 8 to 15 μm when operated at temperatures between 150 and 200 K.

Increasing quantum efficiency is the key to the development of competitive QDIP-based FPAs. Quantum efficiency can be increased by increasing the density of QDs and by enhancing infrared absorption in QD-containing material. QDIPs demonstrated thus far have consisted, variously, of InAs islands on GaAs or InAs islands in InGaAs/GaAs wells. These QDIPs have exhibited low quantum efficiencies because the numbers of QD layers (and, hence, the areal densities of QDs) have been small — typically five layers in each QDIP. The number of QD layers in such a device must be thus limited to prevent the aggregation of strain in the InAs/InGaAs/GaAs non-lattice-matched material system.

The approach being followed in the DWELL-QDIP research is to embed InGaAs QDs in GaAs/AlGaAs multi-quantum-well (MQW) structures (see figure). This material system can accommodate a large number of QD layers without excessive lattice-mismatch strain and the associated degradation of photodetection properties. Hence, this material system is expected to enable achievement of greater densities of QDs and correspondingly greater quantum efficiencies. The host GaAs/AlGaAs MQW structures are highly compatible with mature fabrica-



Quantum Dots Are Embedded in Quantum Wells in a multiple-quantum-well structure. The multiplicity of wells makes it possible to attain a high areal density of QDs for high quantum efficiency.

tion processes that are now used routinely in making QWIP FPAs. The hybrid InGaAs-dot/GaAs/AlGaAs-well system also offers design advantages in that the effects of variability of dot size can be partly compensated by engineering quantum-well sizes, which can be controlled precisely.

Heretofore, a typical QDIP has exhibited high dark current attributable partly to a high-band-gap ohmic contact layer and partly to the fact that because of the low density of QDs, the QDs do not occupy all of the cross section presented to incident light and, hence, some of the current flowing in the device does not pass through the detector material. The undesired effect of the high-band-gap contact layer can be overcome by adding a high-band-gap barrier layer or placing an undoped spacer layer of GaAs, between about 500 and 600 \AA thick between the quantum wells and the top contact layer. It has been previously demonstrated that such spacer layers can significantly reduce tunneling injection currents from contacts to quantum-well regions, thereby reducing dark currents.

Recently, it has been discovered that QDIPs exhibit strong QWIP-like inter-subband absorption. The practical significance of this discovery is that it should be possible to increase the coupling of light into QDIPs, thereby increasing quantum efficiencies, by use of two-dimensional gratings.

This work was done by Sarath Gunapala, Sumith Bandara, David Ting, Cory Hill, John Liu, Jason Mumolo, and Yia Chung Chang of Caltech for NASA's Jet Propulsion Laboratory. Further information is contained in a TSP (see page 1). NPO-43977

In accordance with Public Law 96-517, the contractor has elected to retain title to this invention. Inquiries concerning rights for its commercial use should be addressed to:

*Innovative Technology Assets Management
JPL
Mail Stop 202-233
4800 Oak Grove Drive
Pasadena, CA 91109-8099
(818) 354-2240
E-mail: iaoffice@jpl.nasa.gov
Refer to NPO-42362, volume and number of this NASA Tech Briefs issue, and the page number.*

Integrated Microbatteries for Implantable Medical Devices

Extremely small batteries could operate for years at nanoampere discharge rates.

NASA's Jet Propulsion Laboratory, Pasadena, California

Integrated microbatteries have been proposed to satisfy an anticipated need for long-life, low-rate primary batteries, having volumes less than 1 mm³, to power electronic circuitry in implantable medical devices. In one contemplated application, such a battery would be incorporated into a tubular hearing-aid device to be installed against an eardrum. This device is based on existing tube structures that have already been approved by the FDA for use in human ears.

As shown in the figure, the battery would comprise a single cell at one end of the implantable tube. A small volume of

Li-based primary battery cathode material would be compacted and inserted in the tube near one end, followed by a thin porous separator, followed by a pressed powder of a Li-containing alloy. Current-collecting wires would be inserted, with suitably positioned insulators to prevent a short circuit. The battery would contain a liquid electrolyte consisting of a Li-based salt in an appropriate solvent. Hermetic seals would be created by plugging both ends with a waterproof polymer followed by deposition of parylene.

This work was done by Jay Whitacre and William West of Caltech for NASA's Jet Propul-

sion Laboratory. Further information is contained in a TSP (see page 1).

In accordance with Public Law 96-517, the contractor has elected to retain title to this invention. Inquiries concerning rights for its commercial use should be addressed to:

*Innovative Technology Assets Management
JPL*

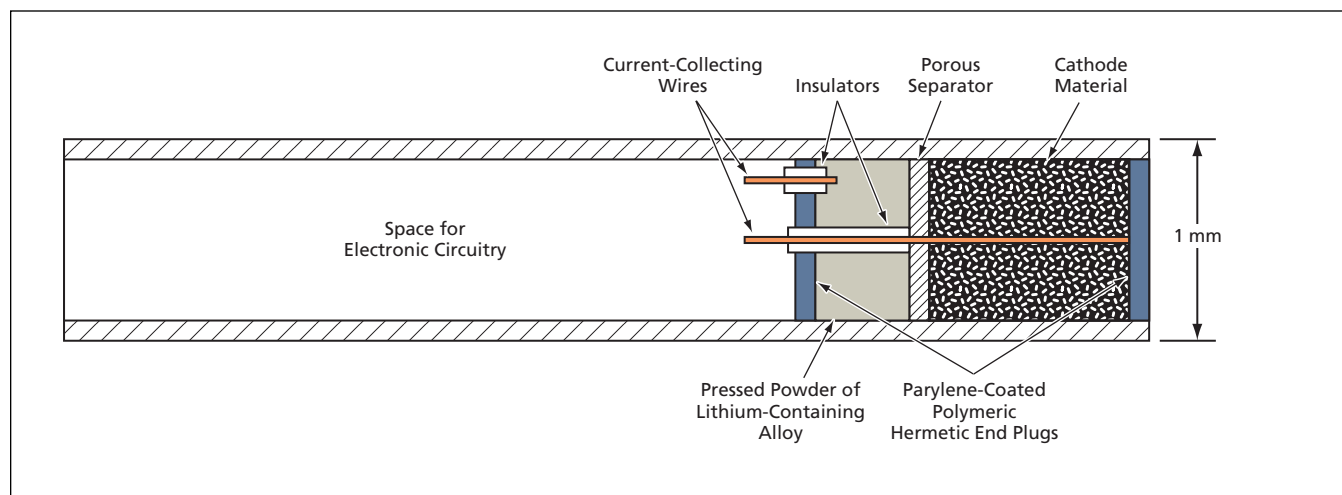
Mail Stop 202-233

4800 Oak Grove Drive

Pasadena, CA 91109-8099

E-mail: iaoffice@jpl.nasa.gov

Refer to NPO-42287, volume and number of this NASA Tech Briefs issue, and the page number.



A **Microbattery Would Be Integrated** into a tubular implantable device. The battery could supply a total charge of about 0.7 mA·h — equivalent to sustaining a discharge current of 80 nA for a year.



Oxidation Behavior of Carbon Fiber-Reinforced Composites

OXIMAP is a numerical (FEA-based) solution tool capable of calculating the carbon fiber and fiber coating oxidation patterns within any arbitrarily shaped carbon silicon carbide composite structure as a function of time, temperature, and the environmental oxygen partial pressure. The mathematical formulation is derived from the mechanics of the flow of ideal gases through a chemically reacting, porous solid. The result of the formulation is a set of two coupled, non-linear differential equations written in terms of the oxidant and oxide partial pressures. The differential equations are solved simultaneously to obtain the partial vapor pressures of the oxidant and oxides as a function of the spatial location and time. The local rate of carbon oxidation is determined at each time step using the map of the local oxidant partial vapor pressure along with the Arrhenius rate equation. The non-linear differential equations are cast into matrix equations by applying the Bubnov-Galerkin weighted residual finite-element method, allowing for the solution of the differential equations numerically.

The mathematical formulation and the numerical solution allow for two types of diffusion: a pressure gradient-driven diffusion (Darcy) and a mass concentration gradient-driven diffusion (Fick). The Darcian flow is governed by the material permeability, and the Fickian flow is governed by the areal porosity and gas diffusivity. OXIMAP allows for orthotropic transport properties, so that the permeability and areal porosity in the two perpendicular directions can have different values. The input into OXIMAP includes: the temperature history, the finite-element nodal coordinates and element connectivity, the material permeability and areal porosity in the principal material directions, the gas viscosity, the volumetric porosity, the initial carbon fiber volume fraction and the initial carbon fiber coating volume fraction, the carbon fiber and carbon fiber coating area fractions, the stoichiometric constants and the Arrhenius constants for the oxidation reaction, and the oxygen and oxide vapor-pressure boundary conditions.

This program was written by Roy M. Sullivan of Glenn Research Center. Further information is contained in a TSP (see page 1).

Inquiries concerning rights for the commercial use of this invention should be addressed to NASA Glenn Research Center, Innovative Partnerships Office, Attn: Steve Fedor, Mail Stop 4-8, 21000 Brookpark Road, Cleveland, Ohio 44135. Refer to LEW-18212-1.

GIDEP Batching Tool

This software provides internal, automated search mechanics of GIDEP (Government-Industry Data Exchange Program) Alert data imported from the GIDEP government Web site. The batching tool allows the import of a single parts list in tab-delimited text format into the local JPL GIDEP database. Delimiters from every part number are removed. The original part numbers with delimiters are compared, as well as the newly generated list without the delimiters. The two lists run against the GIDEP imports, and output any matches. This feature only works with Netscape 2.0 or greater, or Internet Explorer 4.0 or greater.

The user selects the browser button to choose a text file to import. When the submit button is pressed, this script will import alerts from the text file into the local JPL GIDEP database. This batch tool provides complete in-house control over exported material and data for automated batch match abilities. The batching tool has the ability to match capabilities of the parts list to tables, and yields results that aid further research and analysis. This provides more control over GIDEP information for metrics and reports information not provided by the government site.

This software yields results quickly and gives more control over external data from the government site in order to generate other reports not available from the external source. There is enough space to store years of data. The program relates to risk identification and management with regard to projects and GIDEP alert information encompassing flight parts for space exploration.

This program was written by Danny Fong, Dorice Odell, and Peter Barry of Caltech and Tomik Abrahamian of SRS Technologies for NASA's Jet Propulsion Laboratory. Further information is contained in a TSP (see page 1). This software is available for commercial li-

ensing. Please contact Karina Edmonds of the California Institute of Technology at (626) 395-2322. Refer to NPO-43661.

Generic Spacecraft Model for Real-Time Simulation

"Generic Spacecraft" is the name of an evolving library of software that provides for simulation of a generic spacecraft that can orbit the Earth and land on the Moon (and, eventually, on Mars). This library is incorporated into the Langley Standard Realtime Simulation in C++ (LaSRS++) software framework. The generic-spacecraft simulation serves as a test bed for modeling spacecraft dynamics, propulsion, control systems, guidance, and displays.

The Generic Spacecraft library supplements the LaSRS++ framework with an interface that facilitates the connection of new models into the LaSRS++ simulation by eliminating what would otherwise be the necessity of writing additional C++ classes to record data from the models and code to display values on graphical user interfaces (GUIs): The library includes routines for integrating new models into the LaSRS++ framework, identifying model inputs and outputs with full descriptions and units identified, recording data, and automatically generating graphical user interfaces (GUIs). The library is designed to be used in a manner similar to that of LaSRS++ software components for simulating vehicles other than the generic spacecraft. The user specifies (1) a spacecraft and individual models to be constructed and (2) connections between individual model inputs and outputs.

This program was written by Patrick S. Kenney of Langley Research Center and William Ragsdale and Jason R. Neuhaus of Unisys Corp. Further information is contained in a TSP (see page 1). LAR-17534

Parallel-Processing Software for Creating Mosaic Images

A computer program implements parallel processing for nearly real-time creation of panoramic mosaics of images of terrain acquired by video cameras on an exploratory robotic vehicle (e.g., a Mars rover). Because the original images are typically acquired at various camera positions and orientations, it is necessary to

warp the images into the reference frame of the mosaic before stitching them together to create the mosaic. [Also see "Parallel-Processing Software for Correlating Stereo Images," Software Supplement to *NASA Tech Briefs*, Vol. 31, No. 9 (September 2007) page 26.]

The warping algorithm in this computer program reflects the considerations that (1) for every pixel in the desired final mosaic, a good corresponding point must be found in one or more of the original images and (2) for this purpose, one needs a good mathematical model of the cameras and a good correlation of individual pixels with respect to their positions in three dimensions. The desired mosaic is divided into slices, each of which is assigned to one of a number of central processing units (CPUs) operating simultaneously. The results from the CPUs are gathered and placed into the final mosaic. The time taken to create the mosaic depends upon the number of CPUs, the speed of each CPU, and whether a local or a remote data-staging mechanism is used.

This program was written by Gerhard Klimeck, Robert Deen, Michael Mcauley, and Eric De Jong of Caltech for NASA's Jet Propulsion Laboratory.

This software is available for commercial licensing. Please contact Karina Edmonds of the California Institute of Technology at (626) 395-2322. Refer to NPO-30630.

Software for Verifying Image-Correlation Tie Points

A computer program enables assessment of the quality of tie points in the image-cor-

relation processes of the software described in the immediately preceding article. Tie points are computed in mappings between corresponding pixels in the left and right images of a stereoscopic pair. The mappings are sometimes not perfect because image data can be noisy and parallax can cause some points to appear in one image but not the other. The present computer program relies on the availability of a left→right correlation map in addition to the usual right→left correlation map. The additional map must be generated, which doubles the processing time. Such increased time can now be afforded in the data-processing pipeline, since the time for map generation is now reduced from about 60 to 3 minutes by the parallelization discussed in the previous article. Parallel cluster processing time, therefore, enabled this better science result. The first mapping is typically from a point (denoted by coordinates x,y) in the left image to a point (x',y') in the right image. The second mapping is from (x',y') in the right image to some point (x'',y'') in the left image. If (x,y) and (x'',y'') are identical, then the mapping is considered perfect. The perfect-match criterion can be relaxed by introducing an error window that admits of round-off error and a small amount of noise. The mapping procedure can be repeated until all points in each image not connected to points in the other image are eliminated, so that what remains are verified correlation data.

This program was written by Gerhard Klimeck and Gary Yagi of Caltech for NASA's Jet Propulsion Laboratory. Further information is contained in a TSP (see page 1).

This software is available for commercial licensing. Please contact Don Hart of the California Institute of Technology at (818) 393-3425. Refer to NPO-30632.

Flexcam Image Capture Viewing and Spot Tracking

Flexcam software was designed to allow continuous monitoring of the mechanical deformation of the telescope structure at Palomar Observatory. Flexcam allows the user to watch the motion of a star with a low-cost astronomical camera, to measure the motion of the star on the image plane, and to feed this data back into the telescope's control system. This automatic interaction between the camera and a user interface facilitates integration and testing.

Flexcam is a CCD image capture and analysis tool for the ST-402 camera from Santa Barbara Instruments Group (SBIG). This program will automatically take a dark exposure and then continuously display corrected images. The image size, bit depth, magnification, exposure time, resolution, and filter are always displayed on the title bar. Flexcam locates the brightest pixel and then computes the centroid position of the pixels falling in a box around that pixel. This tool continuously writes the centroid position to a network file that can be used by other instruments.

Images are auto-scaled by the program to the screen. Flexcam also allows dark frame, or background frame, subtraction. The centroid of a star's image is computed, while data from ghost images is excluded.

This program was written by Shanti Rao of Caltech for NASA's Jet Propulsion Laboratory.

This software is available for commercial licensing. Please contact Karina Edmonds of the California Institute of Technology at (626) 395-2322. Refer to NPO-44361.



Low-Pt-Content Anode Catalyst for Direct Methanol Fuel Cells

The costs of fuel-cell anodes could be reduced substantially.

NASA's Jet Propulsion Laboratory, Pasadena, California

Combinatorial experiments have led to the discovery that a nanophase alloy of Pt, Ru, Ni, and Zr is effective as an anode catalyst material for direct methanol fuel cells. This discovery has practical significance in that the electronic current densities achievable by use of this alloy are comparable or larger than those obtained by use of prior Pt/Ru catalyst alloys containing greater amounts of Pt. Heretofore, the high cost of Pt has impeded the commercialization of direct methanol fuel cells. By making it possible to obtain a given level of performance at reduced Pt content (and, hence, lower cost), the discovery may lead to reduction of the economic impediment to commercialization.

In the experiments, alloys of various Pt/Ru/Ni/Zr compositions and Pt/Ru compositions were made by co-sputter deposition onto patterned Au on glass substrates at various positions relative to a Pt₄₀Ru₆₀ and Ni₇₀Zr₃₀ sputter targets (the numbers denote atomic percentages). X-ray diffraction analysis of the alloys led to the conclusion that the quaternary alloy most likely consisted of one or two crystalline phases characterized by grain sizes of 1 to 5 nm.

The electrochemical performances of the alloys were tested using both cyclic voltammetry and potentiostatic current measurements. The most promising Pt/Ru/Ni/Zr alloy had a composition of Pt₃₃Ru₂₃Ni₃₀Zr₁₃. Comparative poten-

tiostatic tests of Pt₃₃Ru₂₃Ni₃₀Zr₁₃ and an optimized, state-of-art Pt₈₄Ru₁₆ catalysts were performed (in a solution of 1M

methanol + 1M sulfuric acid at temperatures ranging from 25 to 60 °C). The results of these tests, plotted in the figure, show that the current density [after 5 minutes at 0.7 V vs. NHE (normal hydrogen electrode)] for Pt₃₃Ru₂₃Ni₃₀Zr₁₃ met (as normalized to test structure area), or exceeded (if normalized to surface Pt atoms), the current densities of the state-of-art Pt-Ru under the same test conditions. These data indicate that the new quaternary alloy induced a significantly higher Pt surface site utilization. X-ray photoelectron spectroscopy data indicate that the Pt electron structure in the quaternary material was also very different from that observed in the Pt-Ru alloys.

This work was done by Sekharipuram Narayanan and Jay Whitacre of Caltech for NASA's Jet Propulsion Laboratory. Further information is contained in a TSP (see page 1).

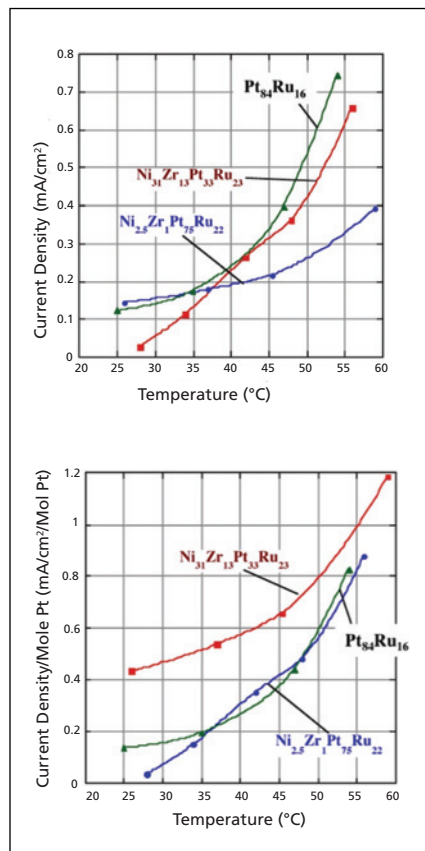
In accordance with Public Law 96-517, the contractor has elected to retain title to this invention. Inquiries concerning rights for its commercial use should be addressed to:

*Innovative Technology Assets Management
JPL*

*Mail Stop 202-233
4800 Oak Grove Drive
Pasadena, CA 91109-8099
(818) 354-2240*

E-mail: iaoffice@jpl.nasa.gov

Refer to NPO-40841, volume and number of this NASA Tech Briefs issue, and the page number.



Plotted Test Results compare current densities for Pt₃₃Ru₂₃Ni₃₀Zr₁₃ with current densities of the state-of-art Pt-Ru under the same test conditions.

Graphite/Cyanate Ester Face Sheets for Adaptive Optics

Unlike glass face sheets, these would be nearly unbreakable.

Marshall Space Flight Center, Alabama

It has been proposed that thin face sheets of wide-aperture deformable mirrors in adaptive-optics systems be made from a composite material consisting of cyanate ester filled with graphite. This composite material appears to offer an attractive alternative to low-thermal-expansion glasses that

are used in some conventional optics and have been considered for adaptive-optics face sheets.

Adaptive-optics face sheets are required to have maximum linear dimensions of the order of meters or even tens of meters for some astronomical applications. If the face sheets were to be made

from low-thermal-expansion glasses, then they would also be required to have thicknesses of the order of a millimeter so as to obtain the optimum compromise between the stiffness needed for support and the flexibility needed to enable deformation to controlled shapes by use of actuators.

It is difficult to make large glass sheets having thicknesses less than 3 mm, and 3-mm-thick glass sheets are too stiff to be deformable to the shapes typically required for correction of wavefronts of light that has traversed the terrestrial atmosphere. Moreover, the primary commercially produced candidate low-thermal-expansion glass is easily fractured when in the form of thin face sheets.

Graphite-filled cyanate ester has relevant properties similar to those of the low-expansion glasses. These properties

include a coefficient of thermal expansion (CTE) of the order of a hundredth of the CTEs of other typical mirror materials. The Young's modulus (which quantifies stiffness in tension and compression) of graphite-filled cyanate ester is also similar to the Young's moduli of low-thermal-expansion glasses. However, the fracture toughness of graphite-filled cyanate ester is much greater than that of the primary candidate low-thermal-expansion glass. Therefore, graphite-filled cyanate ester could be made into nearly

unbreakable face sheets, having maximum linear dimensions greater than a meter and thicknesses of the order of a millimeter, that would satisfy the requirements for use in adaptive optics.

This work was done by Harold Bennett and Joseph Shaffer of Bennett Optical Research, Inc. and Robert Romeo of Composite Mirror Applications, Inc. for Marshall Space Flight Center. For further information, contact Sammy Nabors, MSFC Commercialization Assistance Lead, at sammy.a.nabors@nasa.gov. Refer to MFS-3237-1.

Atomized BaF_2 - CaF_2 for Better-Flowing Plasma-Spray Feedstock

Water atomization is better suited to high-volume production of metal fluoride than conventional methods.

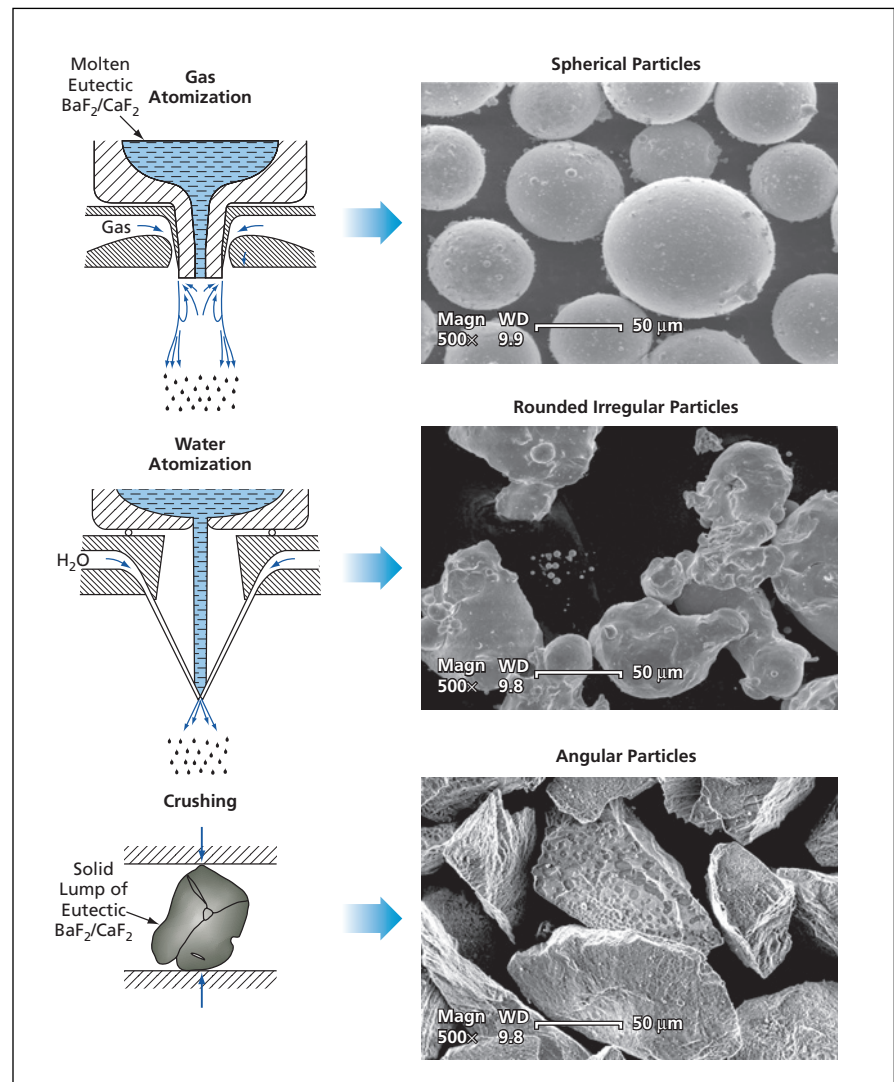
John H. Glenn Research Center, Cleveland, Ohio

Atomization of a molten mixture of BaF_2 and CaF_2 has been found to be superior to crushing of bulk solid BaF_2 - CaF_2 as a means of producing eutectic BaF_2 - CaF_2 powder for use as an ingredient of the powder feedstock of a high-temperature solid lubricant material known as PS304. Developed to reduce friction and wear in turbomachines that incorporate foil air bearings, PS304 is applied to metal substrates by plasma spraying. The constituents of PS304 are:

- An alloy of 80 weight percent Ni and 20 weight percent Cr,
- Cr_2O_3 ,
- Ag, and
- The BaF_2 - CaF_2 eutectic — specifically, 62 weight percent BaF_2 and 38 weight percent CaF_2 .

The superiority of atomization as a means of producing the eutectic BaF_2 - CaF_2 powder lies in (1) the shapes of the BaF_2 - CaF_2 particles produced and (2) the resulting flow properties of the PS304 feedstock powder: The particles produced through crushing are angular, whereas those produced through atomization are more rounded. PS304 feedstock powder containing the more rounded BaF_2 - CaF_2 particles flows more freely and more predictably, as is preferable for plasma spraying.

Two well-known atomization processes (gas atomization and water atomization) have been investigated, in comparison with crushing, as means of producing eutectic BaF_2 - CaF_2 powders (see figure). The particles produced by gas atomization are the most nearly spherical, but each batch contains only a small proportion of particles in the



Water Atomization produces particles intermediate in shape to those produced by gas atomization and crushing. Water atomization may be economically the most advantageous of the three techniques.

size range (20 to 100 μm) suitable for plasma spraying and a much larger proportion of undesired finer particles. Water atomization yields particles that are less spherical in character but still more rounded than those produced by crushing, and yields a greater proportion of usable particles.

As one might expect from the intermediate nature of the shapes of water-atomized $\text{BaF}_2\text{-CaF}_2$ particle shapes, the flow properties of PS304 powders containing water-atomized $\text{BaF}_2\text{-CaF}_2$ are in-

termediate to those of PS304 powders containing equal proportions of gas-atomized $\text{BaF}_2\text{-CaF}_2$ and those containing equal proportions of crushed $\text{BaF}_2\text{-CaF}_2$. Inasmuch as water atomization tends to be less expensive and better suited to high-volume production than is gas atomization, water atomization could be preferable for applications in which the shapes of the eutectic $\text{BaF}_2\text{-CaF}_2$ particles are not required to closely approximate spheres and the intermediate flow properties are acceptable.

This work was done by Christopher Dellacorte of Glenn Research Center and Malcolm K. Stanford of the University of Dayton. Further information is contained in a TSP (see page 1).

Inquiries concerning rights for the commercial use of this invention should be addressed to NASA Glenn Research Center, Innovative Partnerships Office, Attn: Steve Fedor, Mail Stop 4-8, 21000 Brookpark Road, Cleveland, Ohio 44135. Refer to LEW-17709-1.

Nanophase Nickel-Zirconium Alloys for Fuel Cells

Corrosion resistance can be achieved at lower cost.

NASA's Jet Propulsion Laboratory, Pasadena, California

Nanophase nickel-zirconium alloys have been investigated for use as electrically conductive coatings and catalyst supports in fuel cells. Heretofore, noble metals have been used because they resist corrosion in the harsh, acidic fuel-cell interior environments. However, the high cost of noble metals has prompted a search for less-costly substitutes.

Nickel-zirconium alloys belong to a class of base metal alloys formed from transition elements of widely different d-electron configurations. These alloys generally exhibit unique physical, chemical, and metallurgical properties that can include corrosion resistance. Inasmuch as corrosion is accelerated by free-energy differences between bulk material and grain boundaries, it was conjectured that amorphous (glassy) and nanophase forms of these alloys could offer the desired corrosion resistance.

For experiments to test the conjecture, thin alloy films containing various proportions of nickel and zirconium were deposited by magnetron and radio-frequency co-sputtering of nickel and zirconium. The results of x-ray diffraction studies of the deposited films suggested that the films had a nanophase and nearly amorphous character.

For tests of corrosion resistance, films of these alloys were deposited on graphite foils to form working elec-

trodes. In each test, the working electrode was immersed in a 2 N sulfuric acid solution and polarized at a succession of potentials in range of 0.05 to 0.75 V versus a normal hydrogen electrode. The steady-state current sustained by the working electrode was monitored at

one test, part of a nickel foil was coated with this alloy, then the foil was immersed in sulfuric acid for 48 hours. At the end of the test, the alloy coat remained shiny, while the uncoated part of the foil had become corroded. For another test, a thin film of the alloy was

incorporated as a catalyst-support layer in an anode in a fuel cell. The fuel cell was then operated at a temperature of 90 $^{\circ}\text{C}$ for several tens of hours. The fuel cell exhibited stable current densities, indicating that the alloy is stable under fuel-cell operating conditions.

This work was done by Sekharipuram Narayanan, Jay Whitacre, and Thomas Valdez of for Caltech for NASA's Jet Propulsion Laboratory. Further information is contained in a TSP (see page 1).

In accordance with Public Law 96-517, the contractor

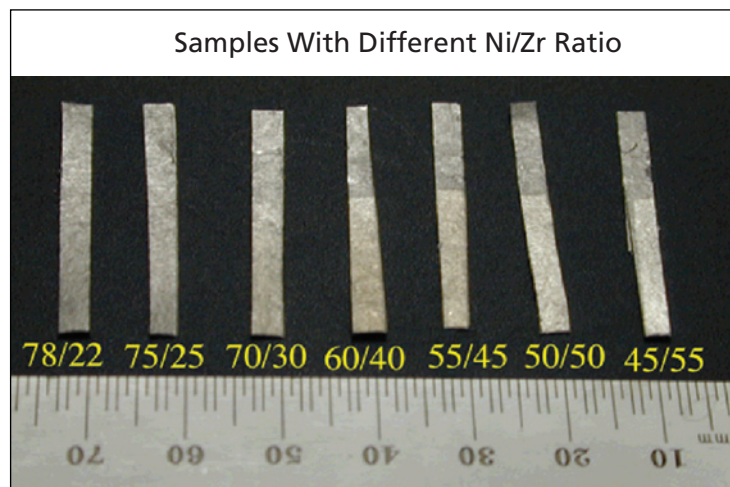
has elected to retain title to this invention. Inquiries concerning rights for its commercial use should be addressed to:

*Innovative Technology Assets Management
JPL*

*Mail Stop 202-233
4800 Oak Grove Drive
Pasadena, CA 91109-8099
(818) 354-2240*

E-mail: iaoffice@jpl.nasa.gov

Refer to NPO-40415, volume and number of this NASA Tech Briefs issue, and the page number.



Samples of Thin Films of Ni/Zr Alloys were photographed after corrosion testing in sulfuric acid. The numbers next to the strips indicate the alloy compositions in atomic percent of Ni/atomic percent of Zr.

each applied potential. For the alloys containing less than 70 atomic percent nickel, the steady-state current densities were less than 1 nA/cm^2 . Inasmuch as current densities less than 100 nA/cm^2 are generally considered indicative of good corrosion resistance, these measurements can be interpreted as indicating excellent corrosion resistance. There was also visual evidence of excellent corrosion resistance (see figure).

One alloy, comprising 55 atomic percent nickel and 45 atomic percent zirconium, was selected for further tests. In



Vacuum Packaging of MEMS With Multiple Internal Seal Rings

Each internal seal ring would be part of an electrical feed-through.

NASA's Jet Propulsion Laboratory, Pasadena, California

A proposed method of design and fabrication of vacuum-packaged microelectromechanical systems (MEMS) and of individual microelectromechanical devices involves the use of multiple internal seal rings (MISRs) in conjunction with vias (through holes plated with metal for electrical contacts). The proposed method is compatible with mass production in a wafer-level fabrication process, in which the dozens of MEMS or individual microelectromechanical devices on a typical wafer are simultaneously vacuum packaged by bonding a capping wafer before the devices are singulated (cut apart by use of a dicing saw). In addition to being compatible with mass production, the proposed method would eliminate

the need for some complex and expensive production steps and would yield more reliable vacuum seals.

Conventionally, each MEMS or individual microelectromechanical device is fabricated as one of many identical units on a device wafer. Vacuum packaging is accomplished by bonding the device wafer to a capping wafer with metal seal rings (one ring surrounding each unit) that have been formed on the capping wafer. The electrical leads of each unit are laid out on what would otherwise be a flat surface of the device wafer, against which the seal ring is to be pressed for sealing. The resulting pattern of metal lines and their insulating oxide coverings presents a very rough and uneven surface, upon which it is diffi-

cult to pattern the sealing metal. Consequently, the seal is prone to leakage unless additional costly and complex planarization steps are performed before patterning the seal ring and bonding the wafers.

In the proposed method, unlike in the conventional method, the electrical leads would not be laid out on the flat sealing surface of the device wafer (see figure). There would be a seal ring surrounding each MEMS or device as in the conventional method, but in addition, there would be smaller internal seal rings (the aforementioned MISRs) within the outer seal ring. Each internal seal ring would be formed integrally with one of the electrical leads of the MEMS or device.

In addition to the conventional processing of the capping wafer, holes concentric with the internal seal rings would be etched through the capping layer. The seal rings would be aligned with the sealing surfaces and the wafers bonded together in a vacuum, as in the conventional method. Then by a combination of electroless plating and electroplating, the through holes would be plated with metal to form electrical feed-throughs that would terminate in the internal seal rings. Hence, each internal seal ring would serve as both (1) part of an electrical feed-through and (2) the vacuum seal for that feed-through.

This work was done by Ken Hayworth, Karl Yee, Kirill Shcheglov, Youngsam Bae, Dean Wiberg, and Chris Peay of Caltech and Anthony Challoner of The Boeing Co. for NASA's Jet Propulsion Laboratory. Further information is contained in a TSP (see page 1).

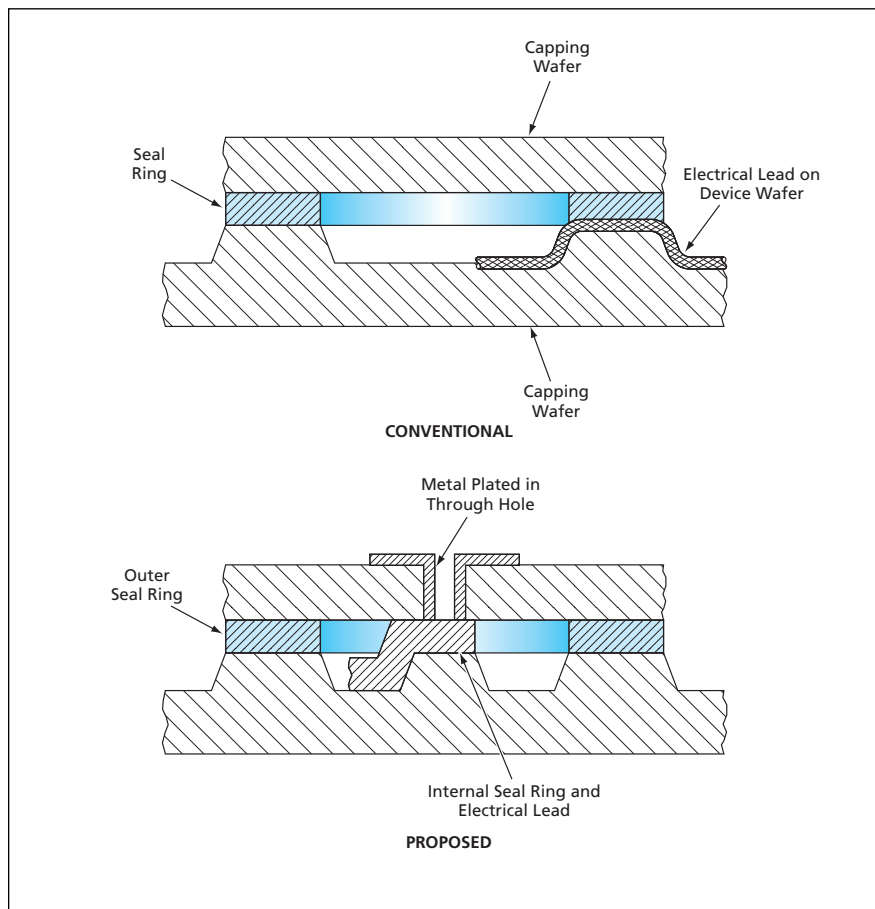
In accordance with Public Law 96-517, the contractor has elected to retain title to this invention. Inquiries concerning rights for its commercial use should be addressed to:

*Innovative Technology Assets Management
JPL*

*Mail Stop 202-233
4800 Oak Grove Drive
Pasadena, CA 91109-8099
(818) 354-2240*

E-mail: iaoffice@jpl.nasa.gov

Refer to NPO-40335, volume and number of this NASA Tech Briefs issue, and the page number.



These Cross Sections of Pertinent Parts of one of many identical devices fabricated on a wafer are greatly simplified in order to illustrate salient differences between the proposed method and the conventional method.



Compact Two-Dimensional Spectrometer Optics

This unit would feature coarse and fine resolution along two orthogonal axes.

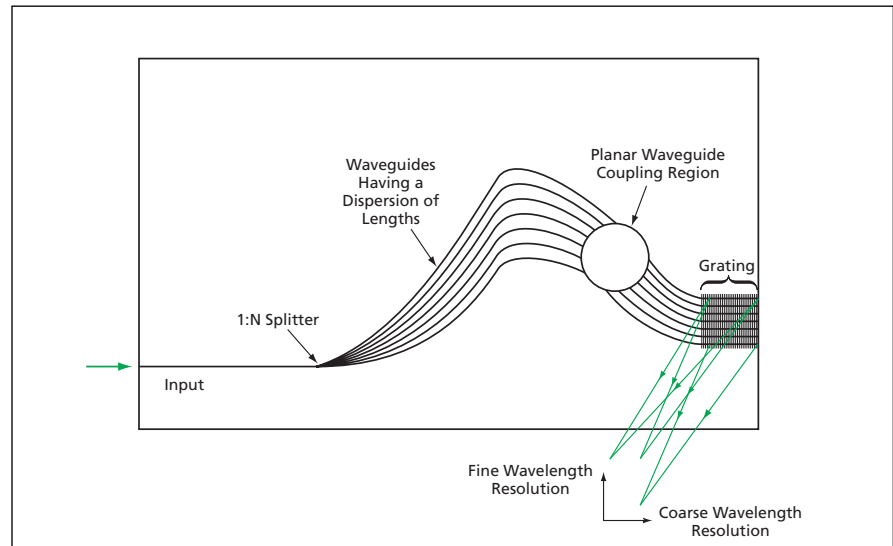
NASA's Jet Propulsion Laboratory, Pasadena, California

The figure is a simplified depiction of a proposed spectrometer optical unit that would be suitable for incorporation into a remote-sensing instrumentation system. Relative to prior spectrometer optical assemblies, this unit would be compact and simple, largely by virtue of its predominantly two-dimensional character.

The proposed unit would be a combination of two optical components. One component would be an arrayed-waveguide grating (AWG) — an integrated-optics device, developed for use in wavelength multiplexing in telecommunications. The other component would be a diffraction grating superimposed on part of the AWG.

The function of an AWG is conceptually simple. Input light propagates along a single-mode optical waveguide to a point where it is split to propagate along some number (N) of side-by-side waveguides. The lengths of the optical paths along these waveguides differ such that, considering the paths in a sequence proceeding across the array of waveguides, the path length increases linearly. These waveguides launch quasi-free-space waves into a planar waveguide-coupling region. The waves propagate through this region to interfere onto an array of output waveguides. Through proper choice of key design parameters (waveguide lengths, size and shape of the waveguide coupling region, and lateral distances between waveguides), one can cause the input light to be channeled into wavelength bins nominally corresponding to the output waveguides.

Notwithstanding the conceptual simplicity as described thus far, the function is complicated by the fact that the response of each output waveguide is char-



A Diffraction Grating Would Be Superimposed on the output portion of an arrayed-waveguide grating in this integrated optical device. The diffraction grating would both (1) impose coarse spectral resolution to break spectral degeneracy and (2) contribute to coupling of light into modes propagating through free space (out of the page).

acterized by a spectral periodicity with multiple frequency components spaced at multiples of the free spectral range appearing in each frequency bin. Hence, in the absence of a corrective measure, each output waveguide would carry multiple wavelength components, resulting in an ambiguous output.

In the proposed device, the degeneracy would be broken by means of the diffraction grating, which would be lithographically formed on the surface in the output waveguide region. The grating lines would cross the output waveguides, establishing orthogonal coordinate axes. One axis would represent coarse spectral resolution; the other, fine spectral resolution. The net result of superimposing the grating on the

output waveguides would be to divert some of the light from waveguide modes to free-space-propagating modes. Because the output diffraction angle of each mode would depend on its wavelength, the output waves propagating in free space would be sorted with coarse spectral resolution along one coordinate axis and fine spectral resolution along the other axis. The proposed unit could be designed, in conjunction with a planar photodetector array, to obtain an optimal match between the array pixel pattern and the wavelength-dispersion pattern.

This work was done by John Hong of Caltech for NASA's Jet Propulsion Laboratory. Further information is contained in a TSP (see page 1). NPO-42431



Fault-Tolerant Coding for State Machines

State machines can be rendered immune to single-event upsets.

NASA's Jet Propulsion Laboratory, Pasadena, California

Two reliable fault-tolerant coding schemes have been proposed for state machines that are used in field-programmable gate arrays and application-specific integrated circuits to implement sequential logic functions. The schemes apply to strings of bits in state registers, which are typically implemented in practice as assemblies of flip-flop circuits. If a single-event upset (SEU, a radiation-induced change in the bit in one flip-flop) occurs in a state register, the state machine that contains the register could go into an erroneous state or could "hang," by which is meant that the machine could remain in undefined states indefinitely. The proposed fault-tolerant coding schemes are intended to prevent the state machine from going into an erroneous or hang state when an SEU occurs.

To ensure reliability of the state machine, the coding scheme for bits in the state register must satisfy the following criteria:

1. All possible states are defined.
2. An SEU brings the state machine to a known state.
3. There is no possibility of a hang state.
4. No false state is entered.
5. An SEU exerts no effect on the state machine.

Fault-tolerant coding schemes that have been commonly used include binary encoding and "one-hot" encoding. Binary encoding is the simplest state machine encoding and satisfies criteria 1 through 3 if all possible states are defined. Binary encoding is a binary count of the state machine number in sequence; the table represents an eight-state example. In one-hot encoding, N bits are used to represent N states: All except one of the bits in a string are 0, and the position of the 1 in the string represents the state. With proper circuit design, one-hot encoding can satisfy criteria 1 through 4. Unfortunately, the requirement to use N bits to represent N states makes one-hot coding inefficient.

Like one-hot encoding, one of the two proposed schemes satisfies criteria 1 through 4. However, the Hamming dis-

State	Binary	One-Hot	Hamming 2	Hamming 3
S0	000	00000001	0000	000000
S1	001	00000010	0011	000111
S2	010	00000100	0101	011001
S3	011	00001000	0110	011110
S4	100	00010000	1001	101010
S5	101	00100000	1010	101101
S6	110	01000000	1100	110011
S7	111	10000000	1111	110100

An Eight-State Example shows different encoding schemes.

tance of 2 encoding is more efficient in that it requires fewer than N bits to represent N states. The scheme is denoted H2 because it requires a Hamming distance of 2 between any two adjacent legal state representations: that is, the strings of bits representing any two adjacent states must differ in two places. Starting from any legal state representation in H2 encoding, an SEU changes the contents of the register to a defined illegal state representation. Because the illegal representation is defined, it can be recognized automatically and used to prevent the state machine from entering an illegal state and from generating incorrect outputs. An H2 code can be generated by adding one additional bit to a binary encoding scheme, as shown in the table.

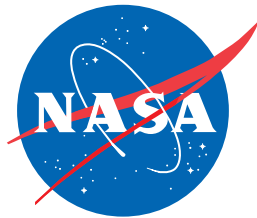
An extension of the H2 concept to require a Hamming distance of 3 between any two adjacent legal state representations yields the H3 coding scheme, which satisfies all five criteria. Starting from any legal state representation in H3 encoding, an SEU changes the contents of the register to a defined illegal state representation that is unique to the legal state representation. Because the illegal representation is defined and associated with one (and only one) legal state representation, it can be recognized automatically and used to restore the state machine to the correct state. The generation

of an H3 code is not as easy as is the generation of an H2 code. An algorithm that generates an H3 code has been devised.

To test these various encodings for fault tolerance, a circuit was devised which could both generate faults and examine the effect of these faults. The circuit was designed to run on an application board containing a Xilinx Spartan II FPGA (field programmable gate array). Hamming-3 (H3) encoding gave by far the best fault tolerance, recording 0 errors in fault injection tests. However, it required the most resources and was the slowest of the encoding methods. Hamming-2 (H2) encoding had fewer errors than binary encoding, but one-hot encoding had the most errors, due to its large number of target flip-flops. It was also the slowest, and showed poor use of resources.

The results from the tests performed showed that for fault-tolerant designs, H2 was the best compromise in terms of size, speed, and fault-tolerance and is preferred over both binary and one-hot state machine encoding. The results also showed H3 encoding to be fault-tolerant to single faults and, therefore, preferred when ultimate reliability is required in a critical application.

This work was done by Stephanie Taft Naegele, Gary Burke, and Michael Newell of Caltech for NASA's Jet Propulsion Laboratory. Further information is contained in a TSP (see page 1). NPO-41050



National Aeronautics and
Space Administration